

# Effect of Average Shear Rate and Impeller Type on the Floc Growth in Stirred Vessels

CHING-JUNG CHUANG\* AND CHANG-LIANG LO

*Department of Chemical Engineering  
Chung Yuan Christian University  
Chung-Li, 32023, Taiwan, R.O.C.*

(Received: December 27, 1999)

## ABSTRACT

Variations of the maximum floc size in the rapid-mixing stages of coagulation and flocculation were analyzed to investigate the effects of average shear rate and type of impeller on floc growth in mixing tanks. Most of the experiments were carried out in a 3.86 liter standard tank with two different impellers: a six-bladed Rushton disk turbine and a 45° pitched-bladed turbine. Detailed floc size measurements indicated that only 10 ~ 20 s of rapid mixing is required and that the differences in performance between the two impellers depend on the average shear rate and the chemical conditions applied. It was suggested that on-line measurement of turbidity can be used to control the impeller speeds for achieving more favorable floc growth.

A theoretical model for relating the maximum size of stable flocs to the impeller speed and floc strength was also presented. Positive correlation has been obtained between this model and the experimental results in literature under a condition of constant adhesive force of flocs. Based on the model and the floc size measurements, the dependence of the adhesive force of flocs after a long period of stirring on the impeller speed was also discussed.

**Key words:** *Coagulation, Flocculation, Floc Size, Rapid Mixing, Stirred Vessel.*

## I. Introduction

Coagulation and flocculation have long been recognized as important pretreatment processes in solid-liquid separation of colloidal suspensions. In these processes relative fluid motion is required to disperse the reagents and enhance the particle-particle collisions. Obviously, at high hydrodynamic stress levels the large aggregates break up again. To maximize the rate of aggregation without rupture as the floc grows in size, the tapered coagulation or flocculation which is subject to high shear briefly applied and then followed by a decrease in the mixing intensity has been widely used in laboratories and industries. Although the tapered shearing paths play vital roles in determining the rate and extent of aggregation[7, 9, 22], no satisfactory criteria for achieving this mixing for ultimate floc growth in stirred vessels have been developed yet. In order to acquire a better understanding of how to achieve an

optimal mixing path in coagulation and flocculation, it is essential to study quantitatively the effects of hydrodynamic stress on the floc growth.

Combinations of stirrers, baffles, and pumps have been used to generate the relative fluid motion in coagulation-flocculation processes. Hoskinson [8] noted that the pumps could not produce satisfactory floc growth because of their very energetic turbulence and quite inhomogeneous distribution of dissipation. When baffled basins are employed for mixing, as Camp[2] has indicated, they are generally unsatisfactory for floc growth by reason of the inhomogeneity and the inability to change mixing intensity under fixed throughput rates.

Although the distribution of kinetic energy is also present in stirred tanks, their flexibility for changing mixing conditions makes them suitable for most coagulation and flocculation processes. Considering the distribution of kinetic energy in stirred tanks, Koh et al.[10] have used

\*To whom correspondences should be addressed.



a compartmentalized model to stimulate the flocculation in stirred tanks and indicated experimentally that the standard mixing flocculators and Couette flocculators both have approximately the same flocculation rate when the same average shear is applied. More recently, Spicer and Pratsinis[16] used the average shear rate to simulate the steady state floc size distribution and the results were in qualitative agreement with experimental data.

Since the flow pattern and power consumption in tanks depend strongly on the impeller designs, Oldshue and Mady [12] have reported on comparisons between the performances of pitched flat-blades, rakes, Rushton turbines, and constant pitch-line velocity impellers on flocculation in water treatment. It appeared that a rake impeller with high power consumption gave the best performance in turbidity removal. Glasgow [6] used Laser-Doppler velocimetry and flow visualization to analyze the hydrodynamic behavior in a rectangular flocculation basin with two different impellers. His results indicated that the perforated paddle, which requires a higher power input, can give a slightly greater floc growth initially than that of a hardware cloth paddle. To the contrary, the latter paddle ultimately produced a larger floc. The effect of stirring intensity on the performance of floc growth was also discussed by Gregory and Guibai[7] concerning flocculating concentrated suspensions in a 1.0 liter beaker with a single-flat blade. The resulting data showed that high mixing intensity can lead to a very fast floc growth initially, but the flocs breakup rapidly and do not reform. Therefore, by reducing the stirrer speed after a few seconds of mixing, great improvement in floc growth can be achieved. Recently, the effect of tank size and impeller geometry on the floc size was studied by Ducoste and Clark[5]. Their results after 30 min of flocculation at an average shear rate of  $40 \text{ s}^{-1}$  indicated the floc size shifts to a small value with increasing tank size and a similar shift was observed when the impeller type was switched from the A 310 foil impeller to the Rushton turbine.

Although studies have been conducted concerning the tapered-shearing paths in the coagulation-flocculation processes to give better floc growth, only a little quantitative information is available concerning determining better operating conditions by adjusting the rapid mixing time and the tapered sequence. In this study a detailed examination of the variations of maximum floc size and turbidity in the rapid-mixing stage was performed to gain insight into achieving the mixing to produce larger flocs. Emphasis was placed on understanding the effects of the average shear rate and impeller design on the floc growth. In addition, the decay in floc size under long periods of stirring was also analyzed to investigate the breakage of flocs in the mixing tanks.

## II. Analysis of floc breakage

Floc growth is controlled not only by the frequency of particle collisions, but also by the ability of flocs to sustain the hydrodynamic stress being exerted on their surfaces. When the adhesive forces between particles within a floc are overcome by the hydrodynamic force, the floc growth is obstructed. Thus, under a given operating condition, there is a maximum stable floc size which is a function of the forces controlling the floc strength and the forces causing rupture. Through a balance between these forces, a variety of theoretical and experimental analyses of maximum stable floc,  $D_{fmax}$ , have been reported [11, 19, 20, 21] and it was generally related to the energy dissipation rate,  $\epsilon$ , of fluids as:

$$D_{fmax} \propto \epsilon^{-n} \quad (1)$$

in which the exponent  $n$  depends on the ratio of the floc size  $D_f$  to the scale of small eddies. (The characteristic size of small eddies in a turbulent flow is generally estimated in the range of the Kolmogoroff microscale,  $\eta$ , defined by:

$$\eta = \left( \frac{\nu^3}{\epsilon} \right)^{1/4}, \text{ where } \nu \text{ is the liquid kinetic viscosity).}$$

Mühle and Domasch[11] have analyzed the maximum stable floc size not only in the ranges of  $D_f \gg \eta$  and  $D_f \ll \eta$  as in previous works, but also in the transition range of  $3\eta < D_f < 58\eta$ . It should be noted that most flocs attained in stirred vessels, in fact, are in the transition range. They considered the binding force,  $B$ , at the plane of rupture within a floc with the average adhesive force between primary particles,  $F_A$ , the floc porosity,  $\epsilon_f$ , and the diameter of primary particle,  $d_p$ , by the following equation:

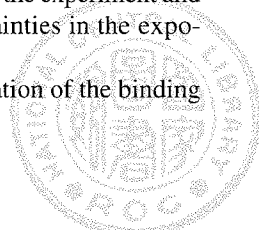
$$B \approx \left( \frac{1 - \epsilon_f}{d_p^2} \right) F_A \quad (2)$$

By balancing the binding force with the hydrodynamic force acting on the floc, a general relationship was established for the maximum stable floc size as

$$D_{fmax} \propto F_A^l d_p^{-m} \epsilon^{-n} \quad (3)$$

The exponents  $l$ ,  $m$  and  $n$  were determined experimentally as (0.50, 1.0, 0.50) and (0.33, 0.66, 0.42) for the cases of  $7\eta < D_f < 58\eta$  and  $3\eta < D_f < 7\eta$ , respectively. Since  $F_A$  in flocs cannot be measured directly, it was determined by the hydrodynamic force required to detach the particles attached to a flat surface by polymer bridging. The differences in surrounding condition between the experiment and a real floc may result in some uncertainties in the exponent values.

Equation(2) implies that an estimation of the binding



# Effect of Average Shear Rate and Impeller Type on the Floc Growth in Stirred Vessels

force requires a knowledge of the floc porosity. In Mühle and Domasch's report  $1-\varepsilon_f \sim \eta D_f^{-1}$  was adopted, but in most studies the floc porosity has been described by the following relationship [1, 4, 18],

$$1 - \varepsilon_f = A D_f^{-K_p} \quad (4)$$

where  $A$  and  $K_p$  are constants dependent on the operating conditions. For clay-alum flocs, the value of  $k_p$  has been reported in the range of 1.0 to 1.5 [18], and increasing with the alum dosage. A similar result of  $K_p = 0.88$  to 1.5 was also presented by Chang [3] for kaolin-flocs formed with both alum and polymer.

By substituting Eq.(4) into (2) and considering the critical condition for floc breakage as  $B \approx D_f^2 \dot{P}_{D_f}$  (where  $\dot{P}_{D_f}$  is the pressure fluctuation on the opposite sides of a floc [20]), the expressions for maximum stable flocs in the range of  $3\eta < D_f < 58\eta$  can be obtained in terms of  $\varepsilon$ ,  $F_A$  and  $K_p$  as

$$D_{fmax} \propto \varepsilon^{-\frac{3}{4(1+K_p)}} F_A^{\frac{1}{1+K_p}} \quad 7\eta < D_f < 58\eta \quad (5)$$

$$D_{fmax} \propto \varepsilon^{-\frac{1}{2+K_p}} F_A^{\frac{1}{2+K_p}} \quad 3\eta < D_f < 7\eta \quad (6)$$

Since the energy dissipation rate in stirred tanks is generally proportional to the 3rd power of the impeller speed, i.e.,  $\varepsilon \propto N^3$ , the above Eqs. with  $K_p$  in the range of 1 to 1.5 can be rewritten as

$$D_{fmax} \propto N^{-(0.9-1.125)} F_A^{(0.4-0.5)} \quad 7\eta < D_f < 58\eta \quad (7)$$

$$D_{fmax} \propto N^{-(0.855-1.0)} F_A^{(0.29-0.33)} \quad 3\eta < D_f < 7\eta \quad (8)$$

Under the restriction of constant  $F_A$ , these relationships were verified by comparison with the experimental results of floc breakage from Chang's [3] study, where the flocs were first prepared under a given operating condition to maintain a constant strength. Then, they were carefully injected into a standard tank to measure the decay of the maximum floc size after a period of stirring. His results for flocs in  $1\eta < D_f < 13\eta$  showed  $D_{fmax} \propto N^{-(0.76-1.13)}$  which compares reasonably well with Eq. (8) under the condition of constant  $F_A$ .

### III. Experimental apparatus and procedures

The experimental set-up is shown in Figure 1a. Floc growth was performed using a four-baffled, 17-cm diameter standard mixing tank. The detailed configurations of the two impellers used for stirring are shown in Figure 1b; one is a six-bladed Rushton disk turbine (abbreviated as RDT in the study), and the other is a 45° pitched-bladed turbine (abbreviated as PBT). The former is a radial flow impeller which provides a strong circulatory flow, whereas

PBT gives axial flow patterns. For these impellers in standard mixing tanks, there are numerous reports concerning the power consumption and flow patterns [13, 14, 15]. In the present study, the average shear rate  $G$  was evaluated by the following equation:

$$G = \sqrt{\frac{P}{\mu V}} \quad (9)$$

in which  $P$  is the power consumption,  $V$  represents the fluid volume, and  $\mu$  denotes the fluid viscosity. Table 1 shows the relationship of the given average shear rate ( $G$ ) to the impeller speed ( $N$ ), the shear rate near the blade tip ( $\gamma_M$ ) [23], and the Kolmogoroff microscale ( $\eta$ ) in the impeller region. For a given average shear rate the PBT impeller requires a higher rotating speed, and the shear rate near the blade tip is approximately two times that in the RDT system. In

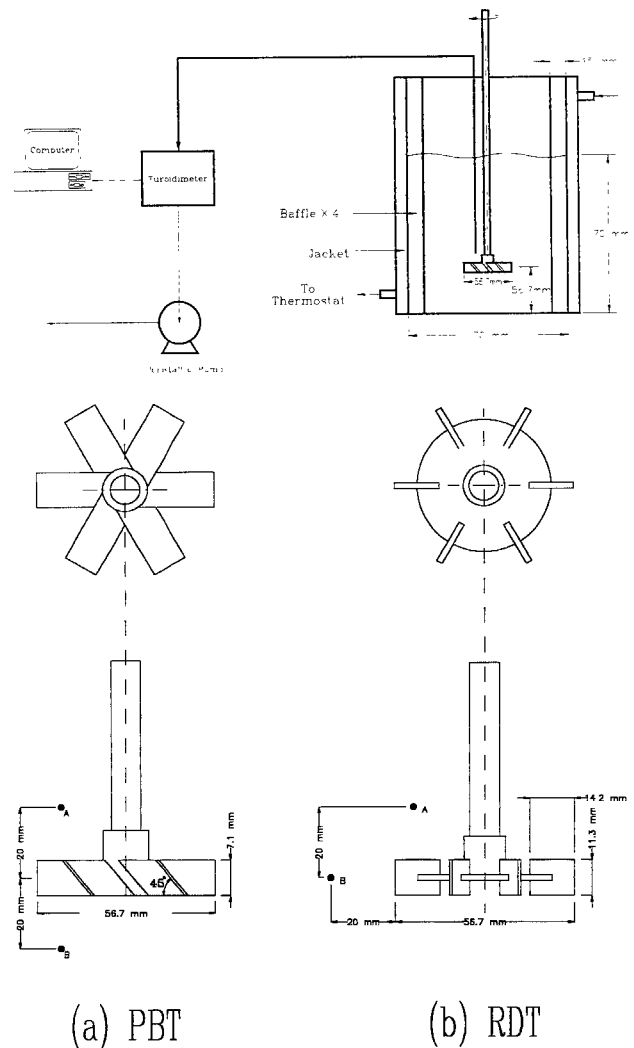
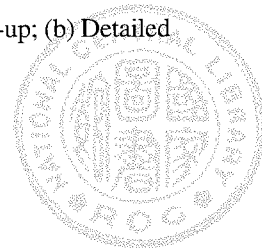


Fig. 1 (a) Scheme of the experimental set-up; (b) Detailed configurations of impellers



**Table 1.** A comparison of  $N$ ,  $\gamma_M$  and  $\eta$  between pitched-bladed and Rushton disk turbines under the same average shear rate

Pitched-bladed turbine				Rushton disk turbine		
$G(s^{-1})$	$N(rpm)$	$\gamma_M(s^{-1})$	$\eta(\mu m)$	$N(rpm)$	$\gamma_M(s^{-1})$	$\eta(\mu m)$
50	145	1342	67	92	678	67
150	302	4034	39	191	2029	39
320	501	8619	26	316	4317	26
650	804	17522	19	507	8774	19

mixing tanks, the breakage of flocs is subject to occur in the impeller region at an extremely turbulent intensity; that is, the floc size is profoundly limited by the local energy dissipation rate  $\epsilon_i$  in the region. According to the studies by Ranade and Joshi [14, 15] in analyzing the energetic efficiency of mixing tanks,  $\epsilon_i$  was estimated at 20 times the average dissipation in the tank. On the basis of  $\epsilon_i = 20 \epsilon$ , the local Kolmogoroff microscales in the impeller region were evaluated and listed in Table 1. For most cases in this study, the ratios of the maximum floc size to the local Kolmogoroff microscale,  $D_{fmax}/\eta$ , are about 1 to 20.

The solid material used in the study was aluminum oxide ( $Al_2O_3$ ) particles, supplied by Alpha Ltd., having the sizes of 0.24 and 2.74  $\mu m$  at the cumulative mass fractions of 10 and 90% respectively, with a median of 0.6  $\mu m$ . Before the experiment in mixing tanks, a jar test was employed to determine the optimal pH value for coagulating the suspension with aluminum sulfate ( $Al_2(SO_4)_3 \cdot 16H_2O$ , abbreviated as alum). It appeared that pH = 6.8 results in a better floc formation and turbidity removal.

The polymeric flocculant used throughout this study was a low cationic polyacrylamide (PAA) with a molecular weight of  $2 \sim 4 \times 10^6$  g mol<sup>-1</sup>, supplied by Chem. Link Ltd. To offer more extension of the polymer branches for bridging, the polymer solutions (100ppm) were prepared 12 hrs before flocculation; by dissolving solid polymer in distilled water under a continuously weak agitation.

At the beginning of the experiments in coagulation, alum was first dispersed in the tank filled with distilled water and, meanwhile, the pH was adjusted by NaOH and  $H_2SO_4$  solutions to remain at 6.8 throughout the processes. Then, under given impeller speeds, 40 ml of a well-dispersed  $Al_2O_3$  suspension was injected by a syringe at a constant rate of 5ml/s to give a final solid concentration of 400 ppm. In the coagulation-flocculation experiments, the polymer solution was injected after 2 min of coagulation to reach a final flocculant concentration of 1.0 ppm. The suspension or polymeric flocculant was injected at a point just above the impellers (point A in Figure 1b).

From the beginning of the process of adding suspen-

sions into the coagulation or adding a polymer solution into the flocculation, a sample of about 25 ml was drawn from the impeller region (point B in Figure 1b) by a 5mm diameter of dipped pipe every 10-20 s. This sample volume was found sufficient to provide reproducible size distribution measurements by Malvern Mastersizer/E, in which a magnetic stirring cell (MSIS) was equipped to prevent the flocs from sedimentation without causing serious floc breakage. The agitated suspension near the impeller region was also drawn continuously by a peristaltic pump to a turbidimeter cell. The turbidity data were recorded by a personal computer. For giving reliable results, 2-3 replicated experiments with a reproducibility error less than 10% were performed.

In this study, additional experiments with a larger tank of 29 cm in diameter were also carried out to investigate the effect of scale-up on the floc growth. Power consumption in the system was determined by direct measurement of the torque on the shaft.

## IV. Results and discussion

### A. Floc sizes from different sampling points

Two points, A and B near the impeller region (see Figure 1b), have been selected for simultaneous sampling to analyze the floc size at different locations. The samples taken from point A are in the circulatory streams flowing into the impeller, and those from point B in the streams

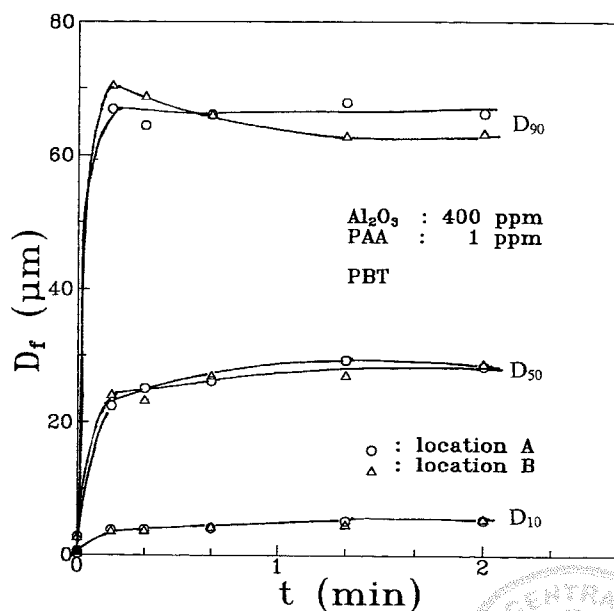


Fig. 2 Variations of floc size from different sampling points near PBT impeller

# Effect of Average Shear Rate and Impeller Type on the Floc Growth in Stirred Vessels

flowing out of the impeller.

Figure 2 shows the variations of floc size,  $D_f$ , in flocculation by PBT with an average shear rate of  $50 \text{ s}^{-1}$ . Because of the limitation of sampling for floc size measurement, the first data was at the 10 s from the start of processing. Here,  $D_k$  was designated as the diameter of flocs to achieve a cumulative mass fraction of  $k\%$ . In the present study,  $D_{90}$  was considered as the size for maximum flocs in a given sample. At the incipient growth of flocs, the high shear in the impeller region enhances the particle aggregations effectively to direct a slightly larger floc in the streams leaving the impeller. Since the shearing also produces the effects of deformation and break-up on large aggregates, after about 30 s of continuous stirring a smaller  $D_{90}$  was observed in the receding streams.

When RDT was used for mixing, there are a shorter path for the circulating streams and a smaller local shear in the impeller region than that stirred by PBT. These factors lead the samples from the two points near RDT to have approximately the same floc size, as shown in Figure 3. The results shown below are all based on the samples from point B, which resides in the circulatory streams departing from the impeller.

## B. Effect of stirring intensity on floc size in PBT system

Figure 4 shows the size of flocs coagulated with a high shear rate ( $G = 650 \text{ s}^{-1}$ ) at two alum dosages, 100 and 500 ppm. In order to understand the floc breakage, the floc size under 15-30 min continuously long stirring was also

measured and shown in the figure. The flocs grew very fast in the initial 10 s up to a size of  $20\text{--}30 \mu\text{m}$ . After this stage further growth was prevented, and a slight decline in floc size occurred in the first 1-2 min of coagulation. With an increase of alum dosage, a faster initial growth rate and larger flocs were obtained, due to the enhancement of the sweeping coagulation by a large amount of aluminum hydroxide ( $\text{Al}(\text{OH})_{3(s)}$ ). Although the alum-coagulated flocs can be reformed after breakage, there is still an obvious reduction in floc size after 15-30 min of continuously strong stirring.

To produce relatively large flocs for rapid settling and/or strong enough to withstand the subsequent dewatering step, a necessary adjunct to coagulation is the addition of a flocculant to bridge the microflocs. A typical floc growth produced by dosing a polymeric flocculant into coagulated suspensions is shown in Figure 5. The peak floc size appears in the initial 10 s with a value about 12 times of the microflocs in the coagulation step; then the floc size decays substantially during the first 2 min of mixing. Although the adding of high alum dosage can increase the peak floc size efficiently, but the large aggregate can't tolerate a high shearing action, due to the hydrodynamic force acting on the floc is proportional to the square of its diameter and on the other hand the flocs containing large amount of aluminum hydroxide are very weak. If the hydrodynamic stress is exerted on the flocs continuously, the polymer branches extending from the floc surfaces compact to lose their bridging ability significantly. The characteristic of being unable to reform after breakage will cause a com-

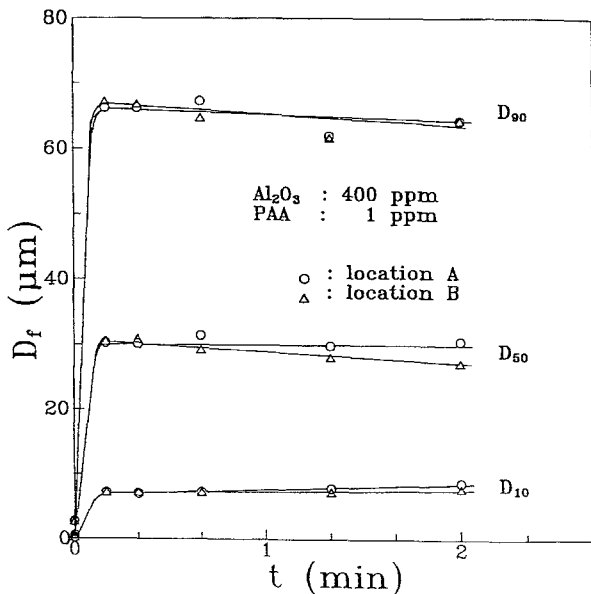


Fig. 3 Variations of floc size from different sampling points near RDT impeller

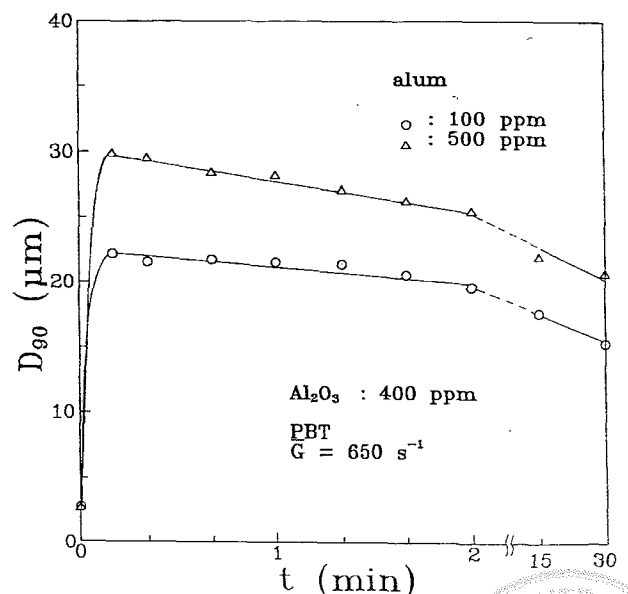
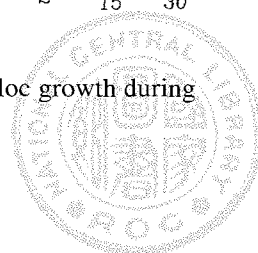


Fig. 4 Effect of alum dosage on the floc growth during coagulation



plete rupture of large aggregates when subjected to a long period of stirring.

Figure 6 shows the effects of shear rate, ranging from  $G = 50$  to  $650 \text{ s}^{-1}$ , on the floc growth in coagulation with 500 ppm alum. Except at a relatively high shear such as  $G = 650 \text{ s}^{-1}$ , larger floc were obtained with a higher stirring

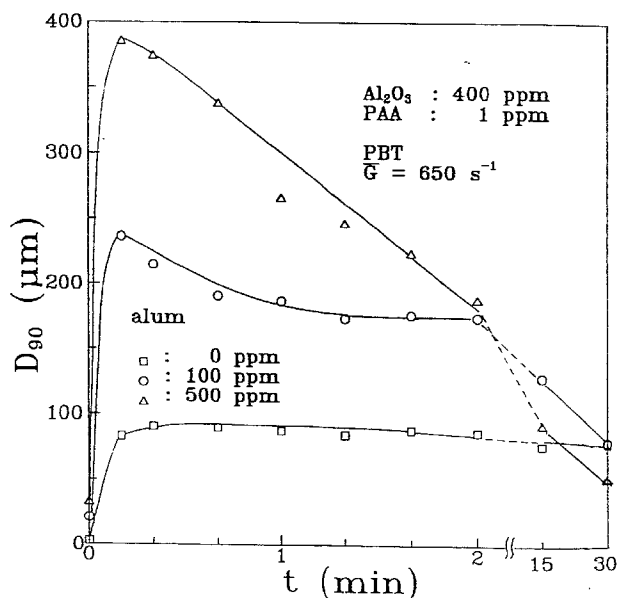


Fig. 5 Effect of alum dosage on the floc growth during flocculation

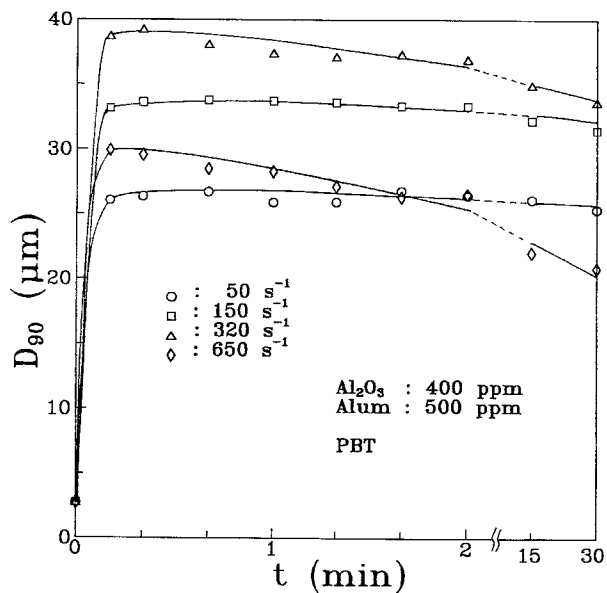


Fig. 6 Effect of average shear rate on the variations of maximum floc size in coagulation (alum 500 ppm, PBT)

intensity. Based on the mechanism of orthokinetic coagulation that the rate of floc growth is proportional to the shear rate when no obvious rupture of flocs occurs [9], the results of smaller flocs obtained initially at the very high shear rate as  $G = 650 \text{ s}^{-1}$  indicate clearly that the hydrodynamic shearing is seriously detrimental for alum-floc growth even only 10 s of stirring. It also appears that, for each given shear rate except  $G$  at  $650 \text{ s}^{-1}$ , there is only a small variation of floc size, which is in consequence of a great ability for the alum-coagulated flocs to reform after breakage.

For the cases in which only a polymeric flocculant was dosed, the floc growth under different degrees of shearing is shown in Figure 7. Because the bridged flocs can sustain a higher hydrodynamic force, even with  $G = 650 \text{ s}^{-1}$  a fast growth rate can be attained at the initial stage of flocculation. However, there is still a distinct decline in floc size after 15~30 min of strong stirring.

For the cases of dosing the flocculant after 2 min of coagulation, the floc growth under four different degrees of agitation is depicted in Figure 8. The formation of microflocs in the coagulation stage can provide an explosive growth of flocs in flocculation. At an average shear rate larger than  $320 \text{ s}^{-1}$ , the rapid dispersion of flocculant and the high frequency of particle collisions make the flocs grow very fast, evidenced by requiring only a short time to reach the peak of  $D_{90}$ . After the peak there is a serious reduction in size, especially with the high shear at  $650 \text{ s}^{-1}$ . This result suggests that only a very short time of about

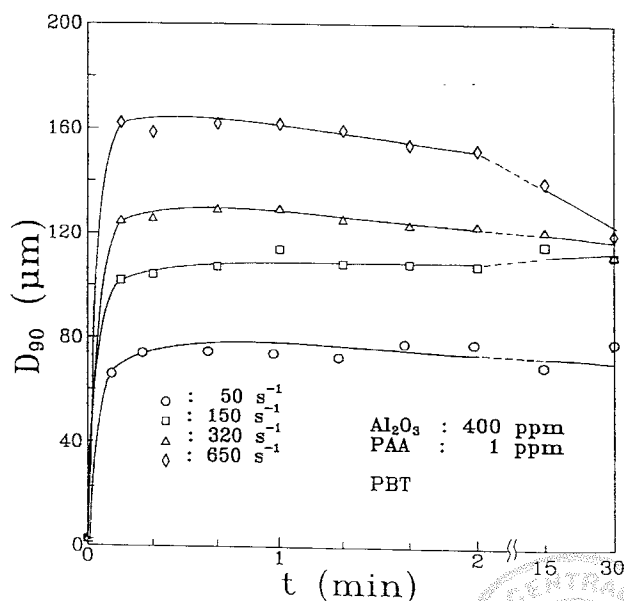


Fig. 7 Effect of average shear rate on the variations of maximum floc size in flocculation (with PBT)

# Effect of Average Shear Rate and Impeller Type on the Floc Growth in Stirred Vessels

10 s is required at the stage of rapid mixing; excess time causes a severely detrimental effect on the ultimate floc size. When a lower shear rate such as 50~150 s<sup>-1</sup> was applied, a longer period of about 20 s of rapid mixing was needed to achieve a better floc growth. Even with a lower shear rate ( $G = 50\text{s}^{-1}$ ), the floc size decreased considerably after 15-30 min of mixing, becoming only slightly larger

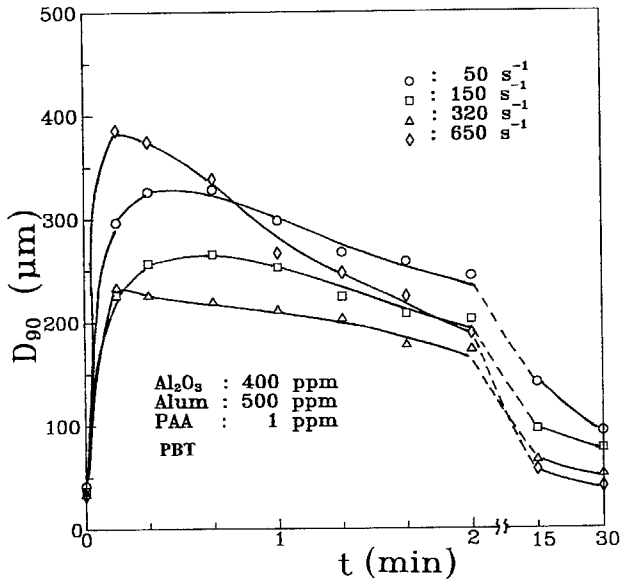


Fig. 8 Floc growth after dosing flocculant into 500 ppm alum-coagulated suspension (with PBT)

than that before flocculation. A regression of the  $D_{90}$  attained after 30 min of agitation gives  $D_{f,max} \sim N^{-0.509}$ , the exponent being only half of that obtained from the theoretical derivations (see Eqs.(8)). Since the theoretical model has been verified above to relate the  $D_{f,max}$  to  $N$  under a condition of constant adhesive force  $F_A$ , thus the difference is obviously by virtue of  $F_A$  not being a constant under a given chemical condition, but as pointed out by Mühle and Domasch[11] being significantly influenced by the hydrodynamic action. Comparing the regression result with Eq.(8) where  $D_{f,max} \propto N^{-1.0}F_A^{0.3}$  was adopted, the relationship of  $F_A$  to the impeller speed was then obtained as  $F_A \propto N^{1.64}$ , which indicates that the  $F_A$  depends importantly on the impeller speed.

## C. Effect of stirring intensity on floc growth in RDT system

For the stirring accomplished by a RDT impeller, the variations of floc size in coagulation are shown in Figure 9. By comparison with that by PBT (see Figure 6), it was found that at  $G = 50\text{--}320\text{ s}^{-1}$  the higher local shear in the PBT region can produce a slightly larger  $D_{90}$ . However, as  $G$  was increased to  $650\text{ s}^{-1}$ , the too-high shear near the PBT blade tip produced opposite results. When the polymer was added into coagulated suspensions, the floc growth by RDT is shown in Figure 10. In comparison with the results in Figure 8, it is apparent that RDT produces larger flocs than PBT. This is caused by the factors that the flocc-

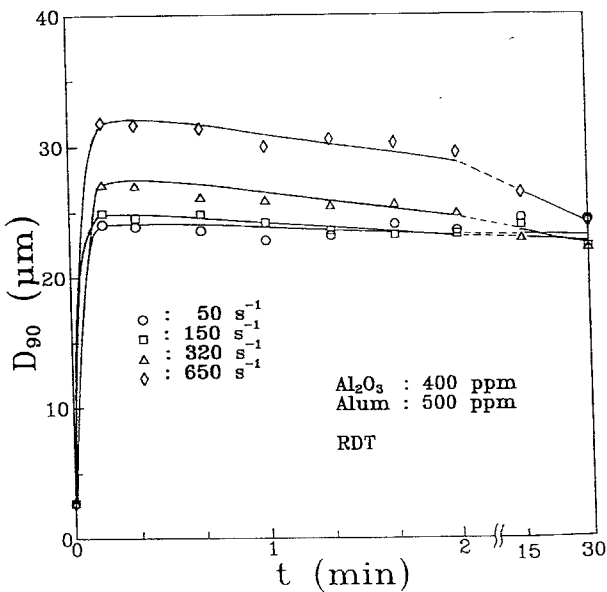


Fig. 9 Variations of maximum floc size by RDT in coagulation with 500 ppm alum

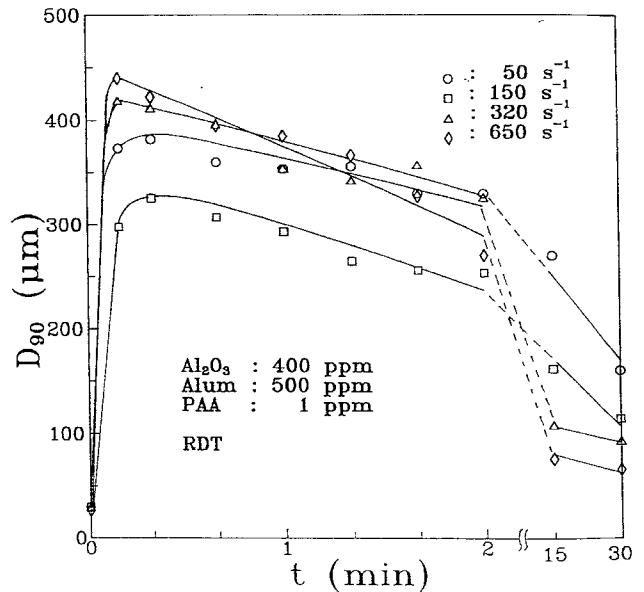
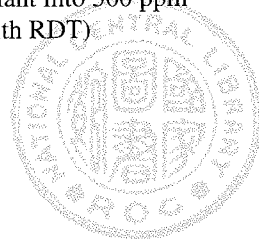


Fig. 10 Floc growth after dosing flocculant into 500 ppm alum-coagulated suspension (with RDT)



culuation of microflocs with an average size of 8~10 μm is controlled by the polymer adsorption and bridging, and the lower local shear in the RDT impeller region giving a more extension of the polymeric branches to bridge microflocs. By relating the floc size after 30 min of stirring by RDT to the impeller speed,  $D_{f,max} \propto N^{-0.51}$  and then  $F_A \propto N^{1.63}$  were obtained when compared with Eq. (8), which is nearly the same as that described above by PBT. The interesting phenomenon of both impellers exhibit similar expression for  $F_A$  versus  $N$  was also observed in other condition as alum 100 ppm and PAA 1.0 ppm, where  $F_A \propto N^{3.61}$  and  $N^{3.52}$  for that by PBT and RDT, respectively. Such results lead to the conclusion that the effect of impeller speed on the adhesive force within flocs after a long period of stirring depends deeply on the chemical condition applied and the difference between the two impellers is not profound under same chemical conditions.

**D. Effect of scale-up on floc growth**

In this research, additional experiments in a larger tank of 19.16 liter were implemented to study the effect of scale-up on floc growth. If the criterion for scale-up is based on the same average shear rate, a lower rotating speed is required in the large tank. When a weak agitation such as  $G = 50 \text{ s}^{-1}$  was applied, it was found that most flocs settle to the bottom of the large tank in the initial stage of flocculation.

Figure 11 shows the time-dependent changes in maximum floc size when flocculation was performed in the large tank. Although the flocs can tolerate 2 min of rapid mix-

ing at a shear rate smaller than  $320 \text{ s}^{-1}$ , it can be seen that 10-20 s of mixing is sufficient for achieving the peak size. By comparison with the results from the small tank (Figure 7), it was found that the large tank can produce considerably larger flocs. Such a tendency was also observed for all other coagulation-flocculation conditions in this study, which is primarily due to that the lower locally turbulence in large tank gives a more extension of polymer branches to bridge aggregates.

**E. Determination of rapid-mixing time for better floc growth**

The results described above indicate clearly that the degree of mixing plays an important role in floc growth. Currently, the criteria for achieving the mixing with regard to ultimate floc growth are generally determined by experienced rules or by a jar test, and 0.5-2 min of rapid mixing is usually adopted in most laboratories and industrial operations. Such a mixing time is too long when compared with the 10-20 s shown in this study. The excess mixing may cause a serious reduction in floc size.

As mentioned above, the information for determining the rapid-mixing time can be provided by measuring the floc size in the initial stage of floc growth. However, the measurement requires 10-30 s for sizing one sample and sometimes causes rupture of aggregates. These shortcomings make this measurement method unsatisfactory when used for on-line control of the impeller speed.

Thus, the variations in turbidity during coagulation and flocculation were also examined to determine the mixing

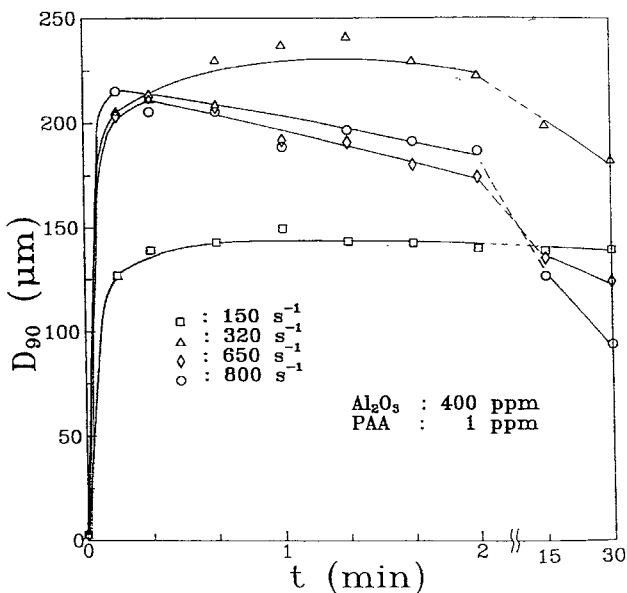


Fig. 11 Floc growth by flocculation in the larger tank

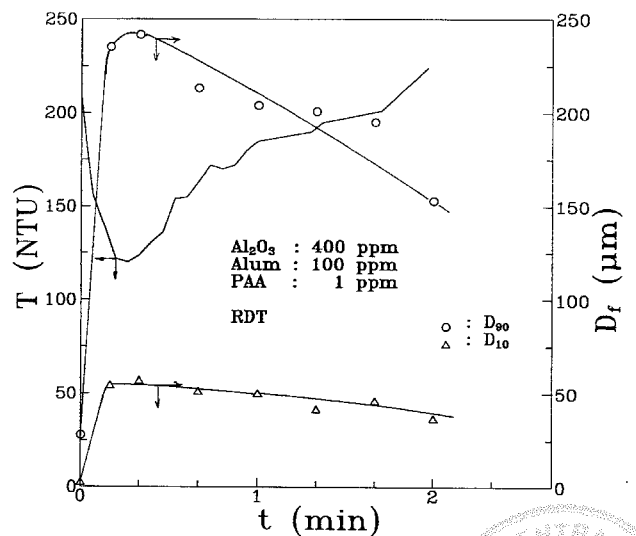
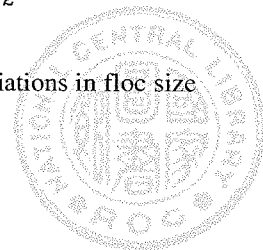


Fig. 12 A comparison between the variations in floc size and in turbidity



# Effect of Average Shear Rate and Impeller Type on the Floc Growth in Stirred Vessels

path. As shown in Figure 12, there is a steep decrease in turbidity in the initial 10 s and, then, a slight increase when the floc size begins to decay. According to this well correspondence between the variations in turbidity and floc size, it can be concluded that the sequences of tapered shearing for better floc growth can be obtained by adjusting the impeller speed to maintain a low turbidity.

## V. Conclusions

Through a detailed examination of the variations in floc size, the effects of average shear rate and impeller design on floc growth in mixing tanks have been investigated. It was found that, under the same average shear rate, the differences in performance between the Rushton disk turbine and the pitched-bladed turbine in floc growth depend on the chemical conditions applied. According to the results that the turbidity data correspond very well with the floc size, a method using on-line detection of turbidity to adjust the impeller speed is proposed to control the ultimate floc growth.

A theoretical model for describing the dependence of maximum stable floc size on the impeller speed and adhesive force,  $F_A$ , within flocs was presented and also demonstrated to be reasonable by comparison with the experimental data available in the literature under the constraint of constant  $F_A$ . Based on this model and the floc size measurements, the dependence of adhesive force within flocs on the impeller speed after a long period of stirring was presented as  $F_A \propto N^\beta$ , where the exponent  $\beta$  varies significantly with the chemical conditions applied and is almost not affected by the impeller designs in the study. Since the floc strength is profoundly influenced by the impeller speeds and chemical conditions and also changed with stirring time, a quantitatively theoretical estimation of maximum floc size in coagulation-flocculation processes still remains as a challenge.

## Acknowledgement

The authors would like to express their gratitude to the National Science Council of R.O.C. for financial support.

## Nomenclature

B: binding force ( $\text{kg}\cdot\text{m}/\text{s}^2$ )  
 $D_{50}$ : median floc size (undersize 50%) (m)  
 $D_{90}$ : undersize 90%(considered as maximum floc size) (m)  
 $D_f$ : floc size (m)  
 $D_{f\max}$ : upper limit of floc size (m)  
 $d_p$ : primary particle size (m)

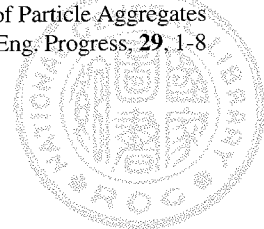
$F_A$ : adhesive force between two particles within a floc ( $\text{kg}\cdot\text{m}/\text{s}^2$ )  
G: average shear rate in a stirred tank ( $\text{s}^{-1}$ )  
N: rotational speed of impellers (rpm)  
P: power transmitted by agitator shaft ( $\text{kg}\cdot\text{m}^2/\text{s}^3$ )  
PAA: polyacrylamide  
PBT: Pitched- blade turbine  
 $p'_{D_f}$ : instantaneous hydrodynamic pressure difference across a floc ( $\text{kg}/\text{m}\cdot\text{s}^2$ )  
RDT: Rushton disk turbine  
T: turbidity, NTU  
t: agitation time (s)

## Greek symbols

$\epsilon$ : mean energy dissipation rate( $\text{m}^2/\text{s}^3$ )  
 $\epsilon_i$ : local energy dissipation rate in the impeller region ( $\text{m}^2/\text{s}^3$ )  
 $\epsilon_f$ : floc porosity  
 $\gamma_M$ : maximum shear rate near the blade tip ( $\text{s}^{-1}$ )  
 $\eta$ : Kolmogorov microscale (small eddy length) (m)  
 $\mu$ : liquid viscosity ( $\text{kg}/\text{m}\cdot\text{s}$ )  
 $\nu$ : liquid kinematic viscosity ( $\text{m}^2/\text{s}$ )  
 $\rho$ : fluid density ( $\text{kg}/\text{m}^3$ )  
 $\sigma$ : mean binding strength with respect to net sectional area of flocs,  $\text{kg}/\text{m}\cdot\text{s}^2$

## References

1. Andreadakis, A.D., Physical and Chemical Properties of Activated Sludge Floc, *Wat. Res.*, **27**, 1707-1714 (1993).
2. Camp, T.R., Flocculation and Flocculation Basins, *ASCE Transactions*, **120**, 1-16 (1955).
3. Chang, C. L., Study of Characteristics of Flocs Breakage in a Stirred Vessel, Master Thesis, Chung Yuan Christian University, Chung Li, Taiwan, R.O.C. (1993).
4. Clark, M.M. and Flora, J.R.V. , Floc Restructuring in Turbulent Mixing, *J. Colloid and Interface*, **147**, 407-421 (1991).
5. Ducoste, J.J. and Clark, M. M., The Influence of Tank Size and Impeller Geometry on Turbulent Flocculation: I. Experimental, **15**, 215-225 (1998).
6. Glasgow, L. A., Aggregate Characteristics and Turbulence in Flocculation Basins, *Chem. Eng. Comm.*, **98**, 155-171 (1990).
7. Gregory, J. and Guibai, L., Effect of Dosing and Mixing Conditions of Polymer Flocculation of Concentrated Suspensions, *Chem. Eng. Comm.*, **108**, 3-21 (1991).
8. Hoskinson, C.M., Mixing, *Journal American Water Works Association*, **28**, 1522-1534 (1936).
9. Ives, K.J., The Scientific Basis of Flocculation, Sijthoff & Noordhoff International Publishers B.V. (1978).
10. Koh, P.T.L., Andrews, J.R.G. and Uhlherr, P.H.T., Flocculation in Stirred Tanks, *Chem. Eng. Sci.*, **39**, 975-985 (1984).
11. Mühle, K. and Domasch, K., Stability of Particle Aggregates in Flocculation with Polymers, *Chem. Eng. Progress*, **29**, 1-8



- (1991).
12. Oldshue, J.Y. and Mady, O.B., Flocculation Performance of Mixing Impellers, Chem. Eng. Progress, 16, 103-108 (1978).
  13. Perry, R.H. and Chilton, C.H., Chemical Engineers Handbook, 6th Ed., McGraw-Hill, Inc. Section 19 (1984).
  14. Ranade, V.V., and Joshi, J.B., Flow Generated by Pitched Blade Turbines I: Measurements using Laser-Doppler Anemometer, Chem. Eng. Comm., **81**, 197-224 (1989).
  15. Randae, V.V. and Joshi, J.B., Flow Generated by a Disk Turbine: Part I Experimental, Trans. IChemE, **68**, 19-33 (1990).
  16. Spicer, P.T. and Pratsinis, S.E., Shear-Induced Flocculation: The Evolution of Floc Structure and the Shape of the Size Distribution at Steady State, Wat. Res., **30**, 1049-1058 (1996).
  17. Flesch, J.C., Spicer, P.T. and Pratsinis, S.E., Laminar and Turbulent Shear-Induced Flocculation of Fractal Aggregates, AIChE J., **45**, 1114-1124 (1999).
  18. Tambo, N. and Watanabe, Y., Physical Characteristics of Floc, I: The Floc Density Function and Aluminum Floccs, Water Res., **13**, 409-419 (1979).
  19. Tambo, N. and Hozumi, H., Physical Characteristics of Floccs-II. Strength of Floc, Water Res., **13**, 421-427 (1979).
  20. Thomas, D.G., Turbulent Disruption of Floccs in Small Particle Size Suspension, AIChE J., **10**, 517-523 (1964).
  21. Tomi, D.T. and Bagster, D.F., The Behaviour of Aggregates in Stirred Vessels. Part I-Theoretical Considerations on the Effect of Agitation, Trans. IChemE, **56**, 1-8 (1978).
  22. TeKippe, R.J. and Ham, R.K., Velocity-Gradient Paths in Coagulation, Jour. AWWA, **63**, 439-447 (1971).
  23. Wichterle, K., Kadlec, M., and Mitschka, L., Shear Rates on Turbine Impeller Blades, Chem. Eng. Comm., **26**, 25-32 (1984).

## 攪拌槽內剪應率與攪拌翼型式 對膠羽成長之影響

莊清榮 羅中良  
中原大學化學工程學系  
台灣省中壢市普仁22號

### 摘要

本研究以實驗分析攪拌混凝槽內最大膠羽粒徑之變化，多數實驗在3.86升之標準攪拌槽配備6片直葉盤式或45°斜葉式等兩型攪拌翼進行。實驗結果顯示，10~20秒之快混時間即形成最大膠羽，隨槽內平均剪應率與混凝化學條件等之改變，不同型式攪拌翼對膠羽成長之影響有明顯差異。本文亦提出可藉由懸浮液濁度偵測來線上控制攪拌翼轉速，以獲致較佳之膠羽成長路徑。

本研究也提出一理論模式，以關聯最大穩定膠羽粒徑與膠羽強度和攪拌翼轉速，經與文獻中強度均一之膠羽的碎裂結果相比較，此模式之適用性獲得驗證。依據此模式與最大穩定膠羽之實驗結果，本文亦探討了經長時間攪拌作用後之膠羽強度與攪拌翼轉速之關係。

**關鍵詞：** 混凝，膠凝，膠羽，快混，攪拌槽。

